STED super-resolved microscopy

Giuseppe Vicidomini¹, Paolo Bianchini² & Alberto Diaspro^{2,3}

Stimulated emission depletion (STED) microscopy provides subdiffraction resolution while preserving useful aspects of fluorescence microscopy, such as optical sectioning, and molecular specificity and sensitivity. However, sophisticated microscopy architectures and high illumination intensities have limited STED microscopy's widespread use in the past. Here we summarize the progress that is mitigating these problems and giving substantial momentum to STED microscopy applications. We discuss the future of this method in regard to spatiotemporal limits, live-cell imaging and combination with spectroscopy. Advances in these areas may elevate STED microscopy to a standard method for imaging in the life sciences.

The stimulated emission depletion (STED) microscope¹ provides spatial resolution well below the limit imposed by the diffraction of light. This breakthrough is obtained by considering the fluorophore as an active element in the image-formation process and not as a simple reporter². The central role of the fluorophore can also be recognized in all the successive super-resolved microscopy (or nanoscopy) techniques that have blossomed over the last decade^{3,4}. Here, by nanoscopy, we refer to all far-field microscopy techniques that, at least in theory, reach diffraction-unlimited resolution⁴.

Nanoscopy techniques resolve features closer than the diffraction limit by transferring the fluorophores transiently into two discernible states⁵—i.e., states with different spectral, temporal or any other detectable response to the illumination (typically a dark OFF and a bright ON state); the transition between distinguishable states allows sequential recording of signal originating from regions of the sample whose size are much smaller than the diffraction limit, down to the region occupied by a single molecule as in SMLM⁶.

In STED microscopy, a fluorescent probe is first excited by light from the ground state (OFF state) to a (singlet) excited-state (ON state), and then it is either de-excited (i) by light, via stimulated emission

(SE), or (ii) spontaneously, via fluorescence emission. To efficiently force a fluorophore to the OFF state, SE has to win the competition with spontaneous emission, which typically occurs within a few nanoseconds after the excitation event (fluorophore's excited-state lifetime). This short temporal window and the small cross-section of SE demand a high flux of stimulating photons. For example, to quench by half the fluorescence of a fluorophore with 4 ns excited-state lifetime and 25 cm²/J stimulated emission cross-section requires 10 MW/cm² light intensity (saturation intensity). A complete quenching requires much higher intensities, which can cause problems such as photobleaching and phototoxicity. As a consequence, STED microscopy was long thought to be incompatible with long-term and live-cell imaging. This incompatibility, together with the high cost and architectural complexity of the early implementations, substantially slowed the growth and dissemination of STED microscopy. The STED microscope was invented in 1994 (ref. 1), but has only gained substantial momentum in the last 10 years⁷. In that time, STED microscopy has given new insights in several fields of the life sciences, has been commercialized by different companies, and has been implemented by many research groups. Nevertheless, much work remains to improve its effective spatial resolution, as well as other important features, such as penetration depth, temporal resolution and range, live-cell compatibility, spectroscopy combination and quantitative analysis.

Here we review the current status of STED microscopy and provide our perspective on the improvements that will allow this technique to be routinely used and to reach its full potential for biological applications.

Basic principles

Diffraction does not allow light to be focused to a volume smaller than roughly one-half of the light wavelength along the lateral directions (x,y) and three times larger along the optical axis $(z)^8$ (around 200 nm and

¹Molecular Microscopy and Spectroscopy, Istituto Italiano di Tecnologia, Genoa, Italy. ²Nanoscopy and NIC@IIT, Istituto Italiano di Tecnologia, Genoa, Italy. 3Department of Physics, University of Genoa, Genoa, Italy. Correspondence should be addressed to G.V. (giuseppe.vicidomini@iit.it).

RECEIVED 14 FEBRUARY 2017; ACCEPTED 23 AUGUST 2017; PUBLISHED ONLINE 29 JANUARY 2018; DOI:10.1038/NMETH.4593

PERSPECTIVE

600 nm, respectively, for visible light). STED microscopy overcomes this diffraction limit by reversibly silencing (depleting) fluorophores at predefined positions of the diffraction-limited excitation regions. Only the nonsilenced fluorophores in the complementary regions emit light, allowing features closer than the diffraction limit to be separated.

In the most typical STED microscopy implementation (Fig. 1a), the fluorescent confinement is obtained by coaligning the Gaussian excitation beam of a scanning microscope with a second beam, called the STED beam, which (i) is tuned in wavelength to de-excite fluorophores via SE and (ii) is engineered in phase and/or polarization to create a doughnut-shaped focal intensity distribution with 'zero'-intensity point in the center. Although the STED beam focal intensity distribution is diffraction limited, high intensities saturate the SE transition and keep virtually all the fluorophores in the ground state (OFF state), except those located in a region around the 'zero'-intensity point, whose size reaches subdiffraction values and decreases with increasing STED beam intensity. Thus, scanning the coaligned beams together across a specimen leads to an image where the (subdiffraction) spatial resolution is given by the size of the effective fluorescent region around the 'zero'.

Theoretically, the resolution of STED microscopy can reach the molecule's size (the ultimate limit of a fluorescent microscope). In practice, it is limited by the signal-to-noise ratio (SNR)⁹; to obtain an effective resolution enhancement, it is important to both generate subdiffraction fluorescent regions across the whole specimen (according to the Nyquist sampling condition) and to register, from all these regions, enough fluorescent photons to obtain good SNR.

SNR is dependent upon the microscope detection efficiency, the fluorophore's brightness and photostability, and the focal intensity distributions of the beams. For maximum SNR, the STED beam and the excitation beam foci must coincide with nanometer precision, and the residual STED beam's intensity in the 'zero'-intensity point must be minimized¹⁰ (Fig. 1b). For a given number of stimulating photons (average intensity of the STED beam), the fluorescence quenching is maximized when all the photons act shortly after the excitation event and before the spontaneous emission (Fig. 1c)¹¹. Maximization of the fluorescent quenching and minimization of photobleaching also depend on the STED beam's wavelength (Fig. 1d); wavelengths close to the peak of the fluorophore's emission spectrum improve the SE cross-section but increase the probability of exciting the fluorophores with the STED beam. Furthermore, any other absorption of the STED beam photons from the fluorophores should be minimized to reduce photobleaching¹². Considering each of these parameters with respect to one another is crucial for optimized STED microscopy.

Free- and auto-beam alignment systems

Because the SNR of a STED microscopy image depends on the coalignment between the STED and the excitation beams, which in most cases use separate optical paths, any thermal drift and/or mechanical vibration limit the effective resolution of the system. A single laser 'source' for both beams (a laser beam combiner or a supercontinuum source) offers an elegant solution to this problem. In this case, the beams are naturally aligned, but it is necessary to have a beam-shaping device that, depending on the wavelength, shapes the intensity distribution at the

focus as Gaussian (for the excitation beam) or as a doughnut (for the STED beam). Two such devices have been implemented: (i) a phase plate which combines different glass materials¹³ and (ii) a combination of conventional and segmented wave plates (easySTED)14. Since the easySTED device can be engineered to have large spectral bandwidths in which the beam remains Gaussian, it has been used for multicolor STED microscopy based on a single STED beam and multiple excitation beams. EasySTED is used in different commercial systems (Supplementary Note 1). It is worth noting that the ideal beam-shaping device should provide multiple and tunable spectral regions for both the excitation and STED beam. A promising solution toward this direction is the use of a q-plate device¹⁵. The q-plate device acts as doughnut converter for a particular spectral bandwidth, which, unlike free-space devices, can be continuously tuned by changing the bias voltage.

Adaptive optics (AO) represents an alternative solution to the coalignment problem. The introduction of a spatial light modulator (SLM) in the path of the STED beam allows the implementation of auto-alignment procedures ¹⁶. Here, the SLM is also used to generate the doughnut focal intensities distribution for the STED beam.

Laser architectures

Lasers are a fundamental consideration in the dissemination of STED microscopy. The complexity, cost and performance of the microscope are laser dependent (**Supplementary Fig. 1**).

Since quenching is optimized when depletion occurs shortly after fluorophore excitation, STED microscopy is typically implemented with synchronized and temporally aligned pulsed lasers (Fig. 1c, pulsed STED microscopy)—the excitation pulses are followed immediately by the depletion pulses. Furthermore, the ideal STED beam must meet different technical demands: (i) peak intensity much greater than 10 MW/cm² (the saturation intensity) to obtain significant resolution enhancement; (ii) high-repetition rate (tens of MHz) for fast imaging; (iii) few hundreds picosecond pulse width to efficiently quench fluorophores and reduce photobleaching; (iv) narrow spectral width to generate a high quality 'zero'-intensity point; (v) ideally, wavelength tunability to match the spectra of many fluorophores. In early STED microscopy, these requirements led to the development of very complex and expensive instruments (Fig. 2a and Supplementary Fig. 1); at the beginning of the 2000s, most STED microscopes used Ti:Sapphire lasers as STED beams, whose pulses required stretching to guarantee a few hundred picosecond pulse width¹⁷ and conversion to the visible range, if imaging with green-yellow fluorophores¹⁸. A second pulsed diode laser electronically synchronized with the Ti:Sapphire laser provided the excitation beam.

More recently, turnkey STED microscopes based on more economical and less elaborate laser architectures have been implemented and commercialized (**Fig. 2b** and **Supplementary Fig. 1**). Pulsed (sub)nanosecond (diode or fiber)^{19–22} lasers have replaced mode-locked lasers as the STED beam. In these implementations the time-gated detection (gated-pulsed STED microscopy; **Fig. 1c** and **Supplementary Note 2**) compensates for the expected reduction in resolution; the longer the depletion pulses, the lower the peak intensity and the lower the fluorescent quenching. Roughly speaking, by removing the fluorescence occurring during the STED beam action, time gating increases

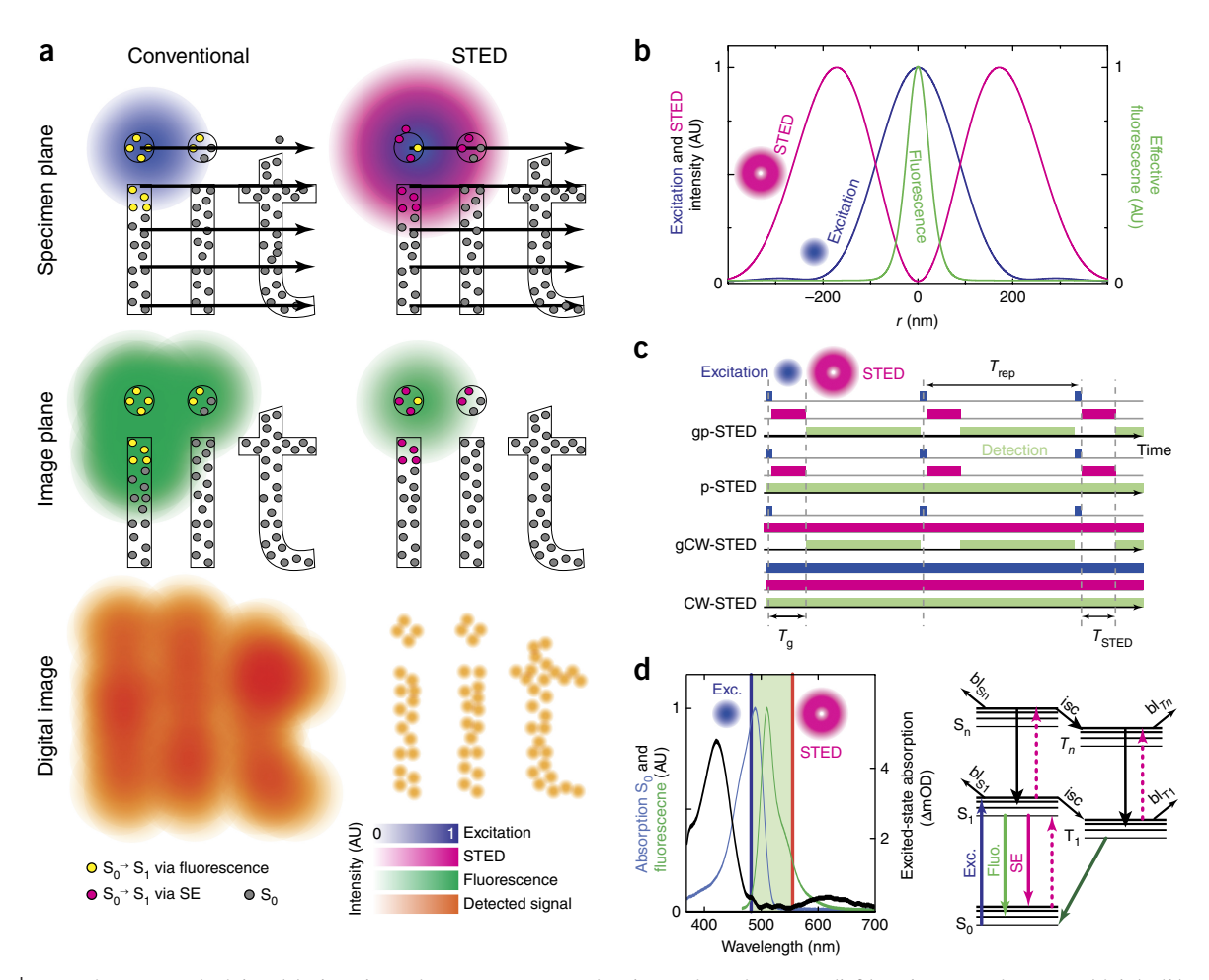


Figure 1 | STED microscopy principles. (a) The schematic compares conventional scanning microscope (left) and a STED microscope (right). (b) Spatial conditions. The maximum and the 'zero' of the excitation and depletion focal intensity distributions, respectively, should coincide. AU, arbitrary units. (c) Temporal conditions. All stimulating photons should act when fluorophores are in the singlet-excited state S₁, and fluorescence must be registered after the stimulating photon's action. Experimental time sequences are shown for the excitation, the depletion, and the fluorescence signal detection for gated pulsed STED (gP-STED), pulsed STED (gP-STED), gated CW-STED (gCW-STED), and CW-STED microscopy. The time-delay $T_{\rm g}$ characterizes the time-gated detection. The pulse-width T_{STED} and the repetition-rate $1/T_{rep}$ characterize the pulsed STED beam. (d) Spectral conditions. All the photons of the STED beam should promote s.e.m. and not be absorbed. Normalized ground-state absorption and fluorescence emission spectra juxtaposed with the excited-state absorption of eGFP81 (left). The Jablonski diagram indicates the transitions relevant for STED microscopy, including the photobleaching (bl) pathways (right). The dashed lines depict unwanted transitions.

the depletion (not the quenching) without increasing the STED beam intensity¹¹. The same principle is at the base of gated continuous wave (CW)-STED microscopy²³ (pulsed excitation and CW depletion; Fig. 1c and Supplementary Note 2), which represents the cheapest and simplest implementation so far. However, the sample is overilluminated—with the CW beam, the stimulating photons also act outside the excited-state fluorophore lifetime, potentially inducing unwanted transitions. It should also be noted that the benefits of time gating come with a reduction in SNR¹¹ (**Supplementary Note 2**).

High-power pulsed supercontinuum laser sources are another important advance in laser technology. The same laser source may provide a synchronized pair of beams (excitation and STED) for any fluorophore^{24,25}. The implementation of STED microscopy based exclusively on these laser sources has been limited by the need to temporally align the excitation and STED beams with an optical delay line, the trade-off between peak intensity and repetition rate, and reduced robustness. However, the most versatile implementations of multicolor STED microscopy are based on a supercontinuum laser for the excitation beam plus a second fiber laser for the STED beam²⁶.

In addition to traditional STED microscopy, two-photon excitation (2PE) STED microscopy is useful for some applications and could be improved by better laser sources. For example, triggerable (sub)nanosecond lasers could overcome limitations in current 2PE STED microscopes²⁶, which rely either on STED beams running in CW, with an overillumination of the sample, or on expensive and sophisticated mode-locked pulsed laser architectures. One unrelated implementation that significantly simplifies 2PE-STED microscopy is the so-called single-wavelength implementation²⁷. However, the use of the same wavelength prevents the simultaneous optimization of the SE and the twophoton absorption cross-sections, and this limits the generality of this implementation.

PERSPECTIVE

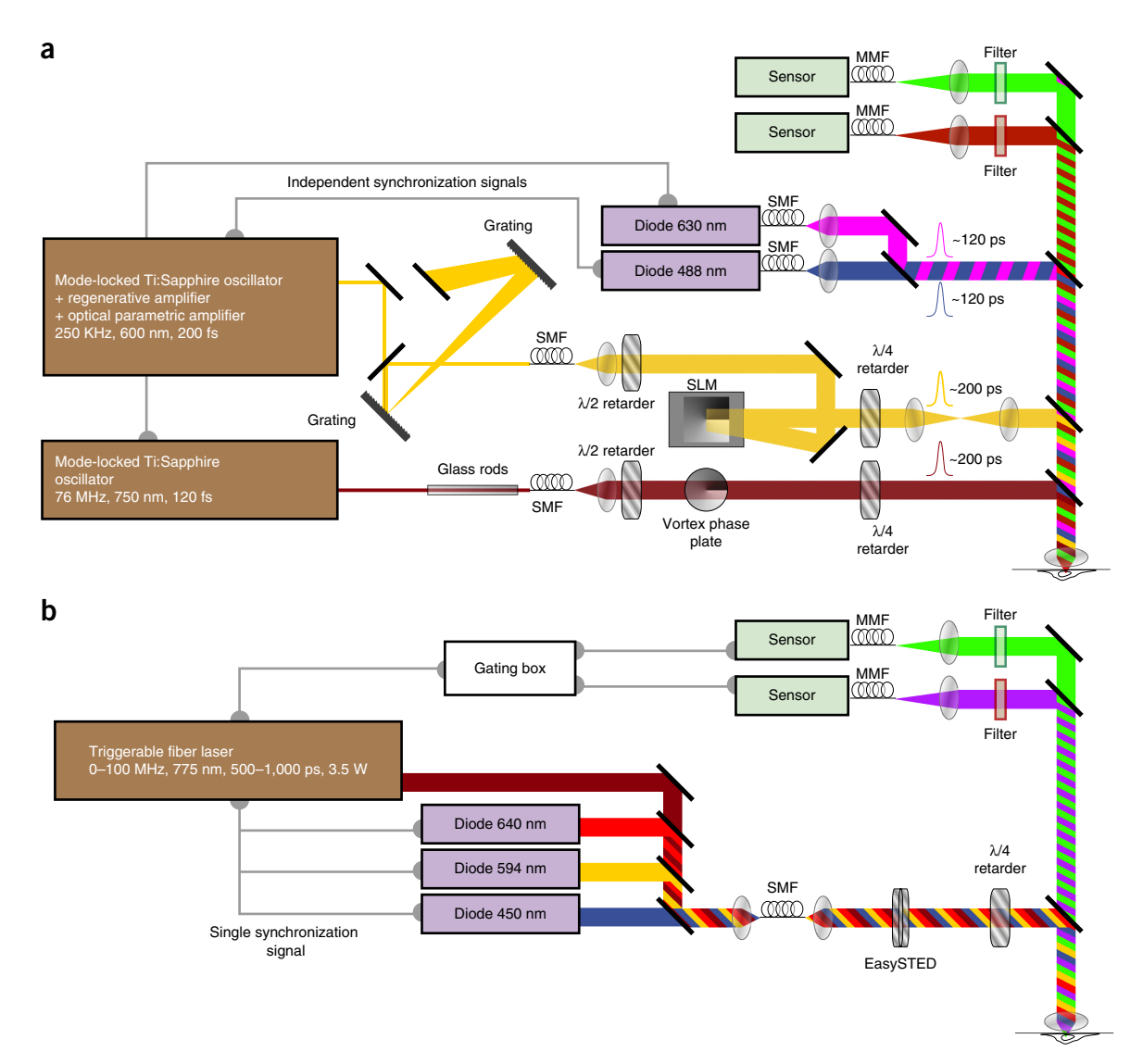


Figure 2 | STED microscopy architectures. (a) In early two-color architecture⁸², every label demanded a pair of laser beams (an excitation and a STED beam). Femtosecond mode-locked Ti:Sapphire lasers provided STED beams where pulses were stretched to hundreds of picoseconds with a combination of gratings, glass roads, and single-mode fibers (SMFs) and, in case of visible fluorophores, converted in wavelength using nonlinear optics. (b) In modern multicolor architectures, long Stokes-shift fluorophores allow use of a single STED beam. A triggerable subnanosecond fiber laser removes the need for pulse preparation, and time-gating detection improves the fluorescent depletion. Subnanosecond lasers provide narrow-band STED beams (<1 nm instead of ~10 nm for the Ti-Sapphire-based STED beam). Combining all the beams into an SMF fiber and using the easySTED device the system is aliqued by design.

Strategies to reduce photobleaching

Each fluorophore has a fixed number of state transition cycles (excitation and de-excitation) that it can undergo before it becomes nonfluorescent through photobleaching. Minimizing photobleaching means that more fluorophores will contribute to SNR and thus resolution, making this a major concern for STED imaging, especially in time-lapse and 3D imaging.

When a fluorophore enters an excited state (singlet or triplet), it has a certain instantaneous probability (rate) to interact with other molecules and produce irreversible covalent modifications that lead to photobleaching (**Fig. 1d**). If the STED beam solely induced SE, it would protect the fluorophore by shortening the singlet excited state duration (thus preventing the crossing to the triplet state). However, in practice, the STED beam induces other

parasitic transitions (**Fig. 1d**), such as the excitation of the fluorophore to higher electronic states (singlet or triplet)¹², from where the rates of photobleaching are even higher. Reducing the population of such higher electronic states reduces photobleaching.

One approach makes use of fluorophores with a low-absorption cross-section at the wavelength of the STED beam (or uses a STED beam at which the fluorophore does not have a high absorption cross-section) and/or of fluorophores having short triplet state lifetimes. These strategies minimize the rate of entering the higher electronic states and the time spent in the triplet state, respectively, thus reducing the overall probability of photobleaching. Although many fluorophores are suitable for STED microscopy, bright and photostable fluorophores, designed specifically for STED microscopy and available across the entire visible spectrum, are still needed.

A promising route for the photostabilization of available fluorescent probes is triplet state quenching²⁸, which is important also from an SNR perspective, since fluorophores in the triplet state are disengaged from the fluorescent cycle.

A second approach minimizes the illumination of the fluorophores while they reside in the triplet state. One implementation uses low-repetition-rate pulsed lasers that allow for an efficient depopulation of any dark state in-between the pulses²⁹. However, lower repetition rates result in increased measurement times. Fortuitously, the same effect can be obtained using ultrafast scanners^{30,31} that enable short pixel dwell time (up to few nanoseconds) and long illumination interleaving period (up to tens of microseconds) without the increase in measurement times. A third approach optimizes the chemicals composing the embedding medium³², such as oxygen scavengers, which, however, could be incompatible with live-cell experiments.

Because excitation and SE are basic transition processes, STED microscopy has also been demonstrated on inorganic nanocrystals, such as nanodiamonds³³, quantum dots (QDs)³⁴ and lanthanide-doped up-conversion nanoparticles (UCNPs)³⁵. Their photostability is typically superior to that of organic compounds, and they have other promising characteristics—for example, UCNPs offer saturation intensity two orders of magnitude lower than those of organics fluorophores. However, application of inorganic nanocrystal as labels is in its infancy compared to organic fluorophores.

Minimizing useless illumination of the fluorophores is another strategy toward the reduction of photobleaching. The so-called RESCue approach³⁶ (Fig. 3a) applies excitation and STED light only at pixels associated with subdiffraction regions effectively containing the fluorophores. In this manner, RESCue avoids additional state transition cycles and thus reduces photobleaching (Fig. 3b). The MINFIELD approach³⁷ is based on a similar idea—by recording only a predetermined subdiffraction-sized area in the sample, fluorophore exposure to the high intensities of the doughnut crest is minimized, and photobleaching is reduced. Recently, the two approaches have been synergistically combined in the DyMIN technique³⁸. In a method called multiple OFF state transitions³⁹ (MOST) or protected STED (Fig. 3a), the fluorophores located in regions subject to excess STED beam intensities (i.e., the doughnut crest) are predriven into a second OFF state that is inert to the excess light. Although this method works only with specific 'photoswitchable' fluorophores, substantial reduction of photobleaching has been demonstrated using reversibly photoswitchable fluorescent proteins (RSFPs) (Fig. 3c).

Finally, time gating opens the possibility to efficiently use long STED beam pulses (CW laser represents the case limit), thus lower peak intensity, to achieve a certain resolution, which mitigates photobleaching⁴⁰.

Live-cell imaging

STED microscopy provides cellular imaging with resolution down to 20 nm²¹. However, whether such results can be achieved in live cells without causing phototoxicity and/or photodamage is an ongoing debate⁴¹. The dose of light needed by the STED beam (up to peak intensities of 1 GW/cm²) to provide resolution in the tens of nanometer is higher than that shown to induce photodamage⁴²; however, multiphoton excitation microscopy, which is considered the method of choice for many *in vivo* applications, normally requires an even

higher dose of light (hundreds of GW/cm²). The compatibility of STED microscopy with live-cell imaging depends on many aspects, such as the wavelength of the STED beam, the time of irradiation, the resolution needed, the investigated area and the specimen itself. Therefore, it is hard to find a general rule for estimating phototoxic effects a priori, and users should carefully and critically examine their sample before and after imaging to verify potential damage⁴³.

Live-cell (and in vivo) STED microscopy imaging using genetically encoded markers such as fluorescent proteins⁴⁴; self-labeling proteins tags⁴⁵ such as SNAP-, HALO- or CLIP-tags; or probes coupled to ligands that specifically bind to a protein of interest have been reported 46,47. In many of these reports, phototoxicity is considered minimal, because cellular substructures such as microtubules showed viable behavior after imaging. But monitoring cell viability only immediately after the irradiation does not exclude light-induced damage, since it has been shown that apoptotic cells still show motility after irradiation, but die some hours later⁴². On the other hand, one might argue that phototoxic effects that manifest themselves after the actual experiment are irrelevant as long as the cellular dynamics during imaging are not disturbed. A rigorous figure of merit to judge damage induced during imaging is still lacking. The first step toward a practical assessment of phototoxicity could be to use a gentler approach, such as differential interference contrast microscopy, to monitor cell morphology, dynamics and growth rate before, during and after STED microscopy, to gauge whether or not they have been altered.

Phototoxicity is highly dependent on the irradiation wavelength; a recent report has shown a massive reduction of phototoxicity when using far-red light instead of visible or ultraviolet (UV) light⁴². Therefore, there is a growing interest to develop photostable far-red live-cell probes^{48,49} or fluorescent proteins⁵⁰ for STED microscopy. A new class of far-red silicon-rhodamine (SiR) probes was recently introduced⁴⁹ that appears to have most of the desirable properties for live-cell imaging—high brightness, fluorogenicity, excellent specificity, cell permeability and high photostability. The potential of SiR dye for live-cell STED microscopy imaging has been demonstrated in combination with selflabeling protein tags 49 . Although self-labeling tags have proven useful, strategies for direct labeling of endogenous proteins would be valuable for a wide range of imaging applications, including STED microscopy. In the case of SiR dye, this problem is solved when the experiment involves the labeling of the microtubules, or the F-actin, or the chromosomal DNA^{46,47}. Unfortunately, these solutions do not extend to all proteins of interest. Nevertheless, the benefits of SiR make it poised to create an entire family of powerful probes for live-cell STED microscopy.

Another important requisite, both for live- and fixed-cell STED microscopy, is the size of the probe. Small probes lead to more accurate subdiffraction images; an antibody has a molecular weight of 150 kDa, a length of 10–15 nm, and the combination of a primary and a secondary antibody is up to 30-nm long. This size is not a problem under the diffraction-limited resolution, but with a resolution of few tens of nanometers, labeling probes of this size cause problems—the fluorophores can be up to 30 nm away from their targets and, because of spatial constraints, the probes will not bind to every target molecule, generating spotty images. Labeling protocols based on SiR probes, aptamers 51 (~15 kDa, ~4 nm) or nanobodies 37 (~13 kDa, ~2–4 nm) satisfy these spatial constraints.

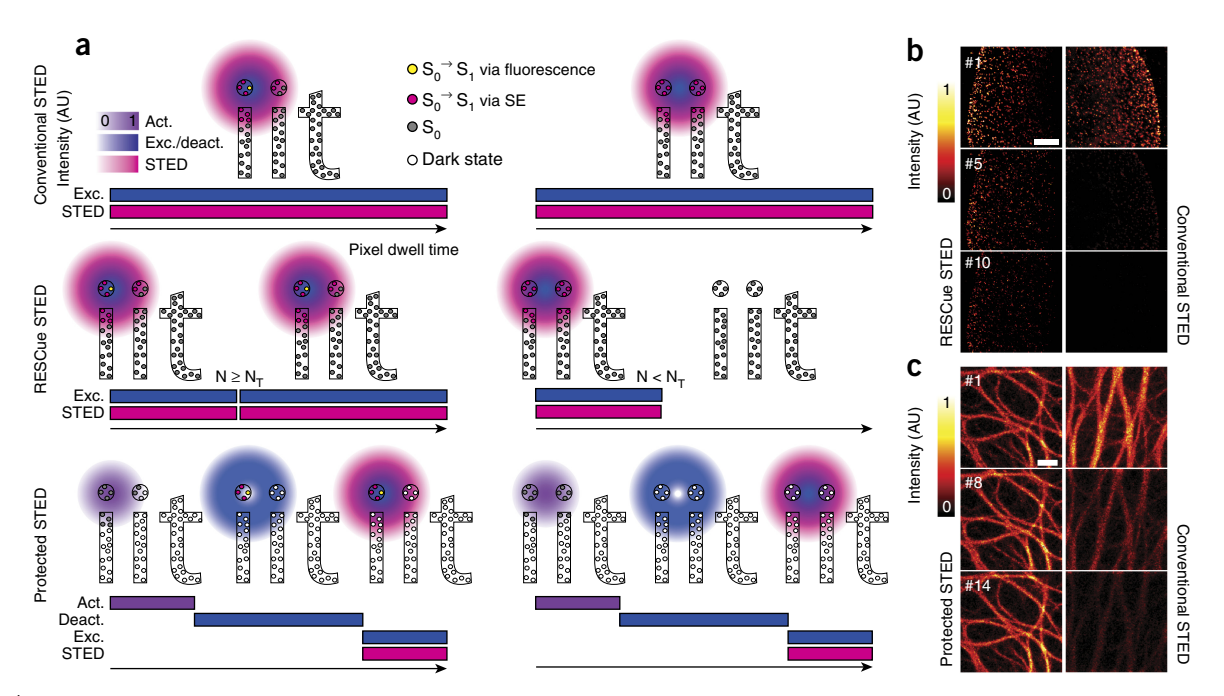


Figure 3 | RESCue- and protected-STED microscopy. (a) The schematic compares conventional (top), RESCue- (middle) and MOST- (bottom) STED microscopy. The RESCue-STED microscope uses a small fraction of the pixel dwell time to determine whether the associated subdiffraction region contains fluorophores (i.e., the photons collected during this fraction N are above a certain threshold N_I); otherwise, the laser beams are shutoff for the rest of the pixel dwell time. The protected-STED microscope uses a fraction of the pixel dwell time to drive fluorophores located on the doughnut crest of the STED beam into a dark state where they do not participate in the excitation and de-excitation cycle. (b) Image series of immunolabeled nuclear pore complex (NPC) subunits in Vero cells for RESCue and conventional STED microscopy. (c) Image series³⁹ of living cells expressing keratin-rsEGFP2 for conventional and protected STED microscopy. Scale bars, 1 μ m.

Phototoxicity is also mitigated using the strategies to reduce photobleaching described above. Photobleaching and phototoxicity mechanisms are strictly connected—when an excited fluorophore interacts with molecules of oxygen in the cellular environment, it undergoes photobleaching, and this reaction can generate toxic free-radical species. As a rule of thumb, photobleaching is a clear indication of phototoxicity, although a lack of photobleaching does not ensure that no phototoxicity has occurred.

Of course, phototoxicity will reduce if the dose of light required to achieve subdiffraction resolution also reduces. Time-gating reduces the peak intensity of the STED beam by one order of magnitude, but a further substantial reduction requires the use of different ON-OFF states, with lifetime longer than the nanosecond lifetime of the excited state. Longer lifetime states reduce the flux of photons required to transfer the fluorophores to another state. At the moment, the most promising class of state transitions for low-illumination nanoscopy is the photoinduced cis-trans isomerizations involving fluorescent and dark isomers. Since these transitions require changes in molecular conformation, the lifetime of the associated states can be very long; RSFPs can be engineered to have millisecond isomeric states 52 . The class of super-resolved techniques involving reversible photoswitching is referred to as reversible saturable optical fluorescence transitions (RESOLFT)⁵³ (Supplementary Note 3).

Three-dimensional imaging

Since samples are inherently 3D, many applications require an isotropic resolution improvement. Notably, the doughnut-shaped STED beam configuration provides resolution enhancement only along the lateral (x,y) direction. Thus, for 3D subdiffraction resolution the focal distribution of the stimulating photons needs to be engineered to form a 'zero'-intensity point surrounded in all directions by regions with high intensity. Currently, two approaches have been followed. The first uses two superimposed incoherent STED beams, one producing the doughnut-shaped focus and confining the fluorescence laterally, and the other producing a bottleshaped focus and confining the fluorescence axially⁵² (**Fig. 4a**). This approach is currently available in different commercial systems (Supplementary Note 1). The second, more technically demanding, superimposes two intensity distributions confining the fluorescence both laterally and axially, but each distribution is obtained from the interference of two coherent beams focused in a 4Pi configuration⁵³ (4Pi-isoSTED microscopy). The 4Pi-isoSTED microscope provides isotropic 3D-resolution of 40 nm, but, since it is based on interference, any changes in the refractive index of the sample may drastically affect the intensity distribution of the stimulating photons, and thus the performance. This condition mainly restricts its application to cells grown in culture.

Another approach to obtain 3D resolution enhancement relies on the integration of the STED principle into light-sheet microscopy (LSM). It has been shown that by integrating a STED beam into a conventional LSM it is possible to enhance its 'axial' resolution⁵⁴, and it has been predicted that both axial and lateral resolutions of a line-scanning LSM can improve if excitation and depletion Bessel beams are used⁵⁵. It would be even more interesting to integrate a STED beam into a lattice LSM⁵⁶—the ability to generate subdiffraction-sized fluorescent 'needles' as well as illumination patterns typical of structured illumination microscopy could trigger a new class of STED architectures that offers 3D resolution enhancement, large field of view and high temporal resolution.

Deep imaging

For 3D applications like tissue or *in vivo* imaging, the resolution improvement must be preserved deep into the samples. Similar to conventional microscopy, light scattering and aberrations are the limiting factors for deep STED microscopy imaging. In addition, scattering and aberrations can break the coalignment of the excitation and STED beams and degrade the quality of the 'zero'intensity point. The first approach for reducing specimen-induced spherical aberration (refractive index mismatch) is the use of a manual correction collar in the objective lens⁵⁷. This approach allows reaching a subdiffraction resolution in living brain slices, but it has been shown to be effective only for 2D STED, where the doughnut-shaped STED beam is less sensitive to aberration compared to the bottle-shaped STED beam. Furthermore, in the case of large-scale 3D images, manual correction at each axial position is unrealistic.

A more general solution, valid both for 2D- and 3D-STED imaging and also able to correct system-induced aberrations, is the use of AO based on deformable mirrors (DMs) and/or SLMs⁵⁸. Whilst AO can mitigate aberrations for deep imaging, the light-scattering problem can be reduced by combining STED microscopy with 2PE microscopy⁵⁹, because the near-infrared (NIR) light of the excitation beam used in 2PE is scattered less by tissues. However, at least at present, most 2PE-STED implementations use a STED beam in the visible region and thus are still affected by strong scattering.

Optical clearing and index matching is a solution that simultaneously minimizes scattering and aberration (from refractive-index mismatching), that is compatible with 2PE-STED and 3D-STED, and that is free from manual or automatic optimization^{60,61}. The limiting factor of this strategy is its incompatibility with living samples.

Fast imaging

Unlike other super-resolved microscopy techniques, STED microscopy drives fluorophores between the ON and OFF states 'instantaneously'; thus, as in confocal microscopy, its temporal resolution is limited technically by the scanning speed and fundamentally by the SNR. In the context of scanning speed, because the gain in spatial resolution is followed by the need for smaller pixel sizes, the recording of large field-of-view requires a large number of pixels, which may decrease the frame rate. However, thanks to recent progress in scanning technology, such as the introduction of resonant scanners³⁰ and electro-optical deflectors³¹, the temporal resolution of a scanning STED microscope already reaches the fundamental limit imposed by the SNR. In other words, the scanning speed is so fast that the pixel dwell time reaches the lifetime of the fluorescent state (a few nanoseconds), but this window typically does not allow for the collection of enough fluorescent photons to build up an image with a good SNR; thus, a number of cumulative frames are necessary.

In the current scenario, where the fluorescent flux is limited, the only way to speed up the time resolution of a point-scanning STED microscope is to either sacrifice the effective resolution or the field of view. For these reasons, currently the most promising approach for fast STED microscopy uses a single spot implementation and moves toward parallelization approaches. One approach implements four cloned excitation and STED beams and four separate point detectors⁶², but the scaling up of this design may be complex.

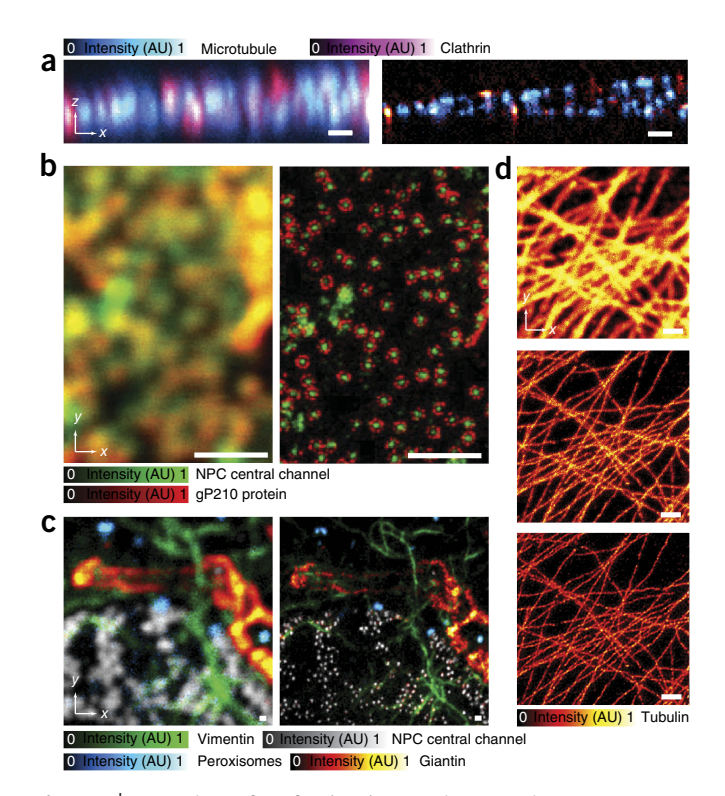


Figure 4 | Comparison of confocal and STED microscopy images. (a) Dual-color 3D confocal (left) and pulsed 3D-STED (right) axial views (x,z) of an immunolabeled fixed cell. (b) Dual-color confocal (left) and pulsed STED (right) images of the immunolabeled subunits in amphibian NPC²¹. (c) Four-color confocal (left) and pulsed STED (right) images of an immunolabeled fixed cell 26 . (d) Single-color confocal (top), gated CW-STED (middle) and deconvolved gated CW-STED (bottom) images of immunolabeled fixed cell⁸³. Scale bars, 1 μm .

A more promising approach uses two orthogonally crossed standing light waves as the depletion pattern and a conventional widefield excitation pattern^{63,64}. Such an optical-depletion pattern features one 'zero'-intensity point per diffraction-limited area; thus, few scanning steps of the 2D periodic pattern yield the full super-resolved image. Because stimulating photons are focused on a relatively larger area with respect to the single-point STED microscope, a critical aspect of parallelization is the need for a high-intensity laser—which, however, can be met by the use of lasers with low repetition rate and high pulse energy.

Combination with spectroscopy

With high temporal resolution and single-molecule sensitivity, fluorescence correlation spectroscopy (FCS) has emerged as an efficient tool for investigating molecular diffusion. But FCS is usually applied on a confocal microscope, and so its observation volume is diffraction limited, and this precludes the resolution of nanoscopic hindrances in molecular diffusion and requires working at nanomolar concentration. The combination of FCS and STED microscopy has solved these limitations—the observation spot in a STED-FCS experiment can be reduced well beyond the diffraction limit⁶⁵. Furthermore, the ability to continuously tune the observation volume from diffraction-size down to tens of nanometers introduces a way of distinguishing between different

DESIGNING A STED MICROSCOPY EXPERIMENT **BOX 1**

When designing a STED microscopy experiment, different aspects have to be considered during sample preparation, imaging and postimaging analysis. Here, we provide brief advice for increasing the success rate of the experiment. We assume the use of a typical commercial scanning STED microscope with basic features (fast scanning, doughnut-based architecture, multicolor).

Sample preparation. (i) Far-red fluorophores reduce scattering, autofluorescence and, in the context of live-cell experiments, phototoxicity. Currently, organic far-red fluorophores combined with self-labeling proteins tags or engineered to specifically bind some subcellular entity are the best choice for live-cell experiments; (ii) regarding photostability and brightness, green-yellow fluorescent proteins are still preferable to red fluorescent proteins; (iii) the most straightforward and reliable multicolor experiment combines long-Stokes shift and normal fluorophores; such a combination provides automatically registered images. In these experiments fluorophores have to be selected for reducing signal cross-talk (microscopy companies provide technical notes suggesting the most suitable dye combinations); (iv) protocols based on small affinity probes instead of conventional antibodies remove artifacts due to probe size hindrance; (v) to avoid optical aberrations the refractive index of the mounting and embedding media required by the objective lens should match, also the thickness of the coverslip must be chosen according to the objective lens specifications. For a thick sample, it may be worth testing clearing solutions.

Imaging. (i) The intensity of the STED beam should be gradually increased until photobleaching starts to appear; (ii) for multicolor experiments with a single STED beam, the excitation wavelengths and the detection spectral windows should be optimized to reduce signal cross-talk. The intensity of the STED beam should be refined for each fluorophore to minimize photobleaching and achieve similar resolution for each color. When available, pixel-by-pixel or line-by-line acquisition schemes should be used to minimize drift between the colors; (iii) short pixel dwell times, such as those provided by a resonant scanner, minimize photobleaching; (v) SNR can be enhanced by line averaging; (vi) if using a pulsed STED beam, the time gating should be delayed no longer than the STED beam pulse width; when using a STED beam running in CW, the time gate should be delayed no longer than half of the fluorophore's excited-state lifetime (this guarantees a signal reduction less than 40%).

Postimaging. (i) If the SNR ratio of a STED image is poor, and/or the STED beam intensity cannot be further increased, an effective resolution enhancement can be obtained using ad hoc image-deconvolution algorithms; however, the restored image has to be critically examined to exclude the introduction of any artifacts; (ii) in a multicolor STED experiment, linear unmixing algorithms should be used only in case of strong cross-talk between the channels; (iii) to exclude phototoxicity during a STED experiment, the vitality of the sample must be investigated both immediately and a few hours after the experiment.

diffusion modes⁶⁶. This capacity has been extensively explored to study 2D molecular dynamics in the cell membrane and recently⁶⁶ has been extended to the study of 3D molecular dynamics in the cytoplasm⁶⁷.

Fluorescence lifetime imaging microscopy (FLIM) is widely used to reveal molecular interactions and environments. When combined with STED microscopy, FLIM can reveal these details at scale of tens of nanometers. However, STED-FLIM analysis is tricky on account of reduced photon counts and perturbation of the fluorophore's lifetime from the STED beam. For a STED beam running in CW, this perturbation makes the analysis nearly impossible. For a pulsed STED beam, it has recently been shown that a pattern-matching approach can compensate for the absence of an accurate model of the photon-arrival-time distribution⁶⁸.

Multicolor imaging is invaluable to understanding how multiple subcellular targets behave or interact. Multicolor STED microscopes have been developed (Fig. 4a-c and Supplementary Fig. 2). Early multicolor STED microscopy was highly complex, since every label needed a pair of laser beams, one to excite and one to deplete (Fig. 2a)⁶⁹. Furthermore, because the more blueshifted STED beam strongly excited the red-shifted label and thus photodamaged it, the choice of labels was restricted, and sequential imaging was necessary. The use of two fluorophores with overlapping emission spectra but with a long (Stokes) shift between the excitation and the emission spectra of one of the fluorophores overcame these problems and reduced the complexity of the architecture (Fig. 2b). In this case, a single STED beam

serves both fluorophores, and the use of two different excitation beams realizes color separation⁷⁰ (Fig. 4a,b). The same concept has recently been extended up to three^{71,72} and four²⁶ (Fig. 4c) fluorophores. Unfortunately, not many long-Stokes-shift fluorophores with high photostability exist; thus, the design of new fluorophores that meet this requirement may boost the multicolor ability of STED microscopy⁷³. At the same time, linear unmixing algorithms increase the number of fluorophore combinations compatible with multicolor STED microscopy. It has been shown that rigorous linear unmixing with a single excitation and a single STED beam can separate two fluorophores^{74,75}.

Summary and outlook

STED has the potential to become a method of choice for studying subcellular structures on the nanoscale. Most of the early developments focused on pushing the resolution to the ultimate limit at the expense of other important properties, such as versatility, temporal resolution, depth imaging and invasiveness. In the last few years, the trend has changed, and many technological advances have partially recovered these properties. This trend is demonstrated by the emergence of new commercial STED microscopes (Supplementary Note 1) and, most importantly, by a series of successful experiments based on STED microscopy (Box 1). However, the gap to satisfy all the needs of the life scientists is still large, and only a synergistic combination of achievements in different fields can fill it. We have here described how (i) new optical devices and lasers transformed STED microscopy into a

turnkey system; (ii) adaptive optics approaches and near-infrared proteins/probes could improve STED imaging depth in tissue; (iii) parallelization via multiple subdiffraction fluorescent regions could speed up STED imaging; (iv) new probes, labeling protocols and imaging scheme can reduce photobleaching and phototoxicity for long-term and live-cell imaging; (v) new probes and imaging schemes could simplify multicolor STED imaging.

In the context of quantitative imaging, it is important to point out that the STED microscope is a linear system, meaning that the signal recorded from a STED microscope in a well-defined subdiffraction volume is proportional to the fluorescent molecule concentration within the volume (apart from photobleaching). Therefore, similar to SMLM, there are no fundamental limits in counting molecules within a particular subcellular structure. Toward this, fluorescence intensity distribution analysis (FIDA) has been combined with STED-FCS⁷⁶ and photon-bunching measurement with STED imaging⁷⁷. We expect that, in the future, assays to map the number of proteins at the nanoscale, also with the help of correlating information from other microscopy techniques⁷⁸, would be a major thrust.

Another important consequence of the linearity of STED microscopy is its compatibility with image restoration and deconvolution⁷⁹ (Fig. 4d and Supplementary Note 4), which can represent a reliable approach to increase the effective resolution without increasing the STED beam intensity⁸⁰. One may envision novel STED microscopy implementations able to probe the molecular organization and dynamics of the cell with a spatiotemporal resolution that can help researchers decipher the most puzzling mechanisms of life.

Note: Any Supplementary Information and Source Data files are available in the online version of the paper.

ACKNOWLEDGMENTS

We equally acknowledge S. Koho, M. Castello and G. Tortarolo (Istituto Italiano di Tecnologia) for fruitful discussions.

COMPETING FINANCIAL INTERESTS

The authors declare no competing financial interests.

Reprints and permissions information is available online at http://www.nature. com/reprints/index.html. Publisher's note: Springer Nature remains neutral with regard to jurisdictional claims in published maps and institutional affiliations.

- Hell, S.W. & Wichmann, J. Breaking the diffraction resolution limit by stimulated emission: stimulated-emission-depletion fluorescence microscopy. Opt. Lett. 19, 780-782 (1994).
- Hell, S.W. Microscopy and its focal switch. Nat. Methods 6, 24-32
- Diaspro, A. ed. Nanoscopy and Multidimensional Optical Fluorescence Microscopy (Chapman and Hall/CRC, 2010).
- Eggeling, C., Willig, K.I., Sahl, S.J. & Hell, S.W. Lens-based fluorescence nanoscopy. Q. Rev. Biophys. 48, 178-243 (2015).
- Hell, S.W. Far-field optical nanoscopy. Science 316, 1153-1158 (2007).
- Klein, T., Proppert, S. & Sauer, M. Eight years of single-molecule localization microscopy. Histochem. Cell Biol. 141, 561-575 (2014).
- Bianchini, P. et al. STED nanoscopy: a glimpse into the future. Cell Tissue Res. 360, 143-150 (2015).
- Born, M. & Wolf, E. Principles of Optics (Cambridge University Press,
- Tortarolo, G., Castello, M., Diaspro, A., Koho, S. & Vicidomini, G. Evaluating image resolution in STED microscopy. Optica 5, 32-35 (2018).
- Galiani, S. et al. Strategies to maximize the performance of a STED microscope. Opt. Express 20, 7362-7374 (2012).
- Vicidomini, G. et al. STED nanoscopy with time-gated detection: theoretical and experimental aspects. PLoS One 8, e54421 (2013).

- 12. Hotta, J. et al. Spectroscopic rationale for efficient stimulated-emission depletion microscopy fluorophores. J. Am. Chem. Soc. 132, 5021-5023 (2010).
- 13. Wildanger, D., Bückers, J., Westphal, V., Hell, S.W. & Kastrup, L. A STED microscope aligned by design. Opt. Express 17, 16100-16110 (2009).
- 14. Reuss, M., Engelhardt, J. & Hell, S.W. Birefringent device converts a standard scanning microscope into a STED microscope that also maps molecular orientation. Opt. Express 18, 1049-1058 (2010).
- Yan, L. et al. Q-plate enabled spectrally diverse orbital-angular-momentum conversion for stimulated emission depletion microscopy. Optica 2, 900-903
- 16. Gould, T.J., Kromann, E.B., Burke, D., Booth, M.J. & Bewersdorf, J. Autoaligning stimulated emission depletion microscope using adaptive optics. Opt. Lett. 38, 1860-1862 (2013).
- 17. Klar, T.A., Jakobs, S., Dyba, M., Egner, A. & Hell, S.W. Fluorescence microscopy with diffraction resolution barrier broken by stimulated emission. Proc. Natl. Acad. Sci. USA 97, 8206-8210 (2000).
- Willig, K.I. et al. Nanoscale resolution in GFP-based microscopy. Nat. Methods 3, 721-723 (2006).
- 19. Westphal, V., Blanca, C.M., Dyba, M., Kastrup, L. & Hell, S.W. Laser-diodestimulated emission depletion microscopy. Appl. Phys. Lett. 82, 3125
- 20. Rankin, B.R., Kellner, R.R. & Hell, S.W. Stimulated-emission-depletion microscopy with a multicolor stimulated-Raman-scattering light source. Opt. Lett. 33, 2491-2493 (2008).
- Göttfert, F. et al. Coaligned dual-channel STED nanoscopy and molecular diffusion analysis at 20 nm resolution. Biophys. J. 105, L01-L03
- 22. Bottanelli, F. et al. Two-colour live-cell nanoscale imaging of intracellular targets. Nat. Commun. 7, 10778 (2016).
- Vicidomini, G. et al. Sharper low-power STED nanoscopy by time gating. Nat. Methods 8, 571-573 (2011).
- 24. Wildanger, D., Rittweger, E., Kastrup, L. & Hell, S.W. STED microscopy with a supercontinuum laser source. Opt. Express 16, 9614-9621 (2008).
- Bückers, J., Wildanger, D., Vicidomini, G., Kastrup, L. & Hell, S.W. Simultaneous multi-lifetime multi-color STED imaging for colocalization analyses. Opt. Express 19, 3130-3143 (2011).
- Winter, F.R. et al. Multicolour nanoscopy of fixed and living cells with a single STED beam and hyperspectral detection. Sci. Rep. 7, 46492 (2017).
- 27. Bianchini, P., Harke, B., Galiani, S., Vicidomini, G. & Diaspro, A. Singlewavelength two-photon excitation-stimulated emission depletion (SW2PE-STED) superresolution imaging. Proc. Natl. Acad. Sci. USA 109, 6390-6393
- 28. van der Velde, J.H.M. et al. A simple and versatile design concept for fluorophore derivatives with intramolecular photostabilization. Nat. Commun. 7, 10144 (2016).
- Donnert, G. et al. Macromolecular-scale resolution in biological fluorescence microscopy. Proc. Natl. Acad. Sci. USA 103, 11440-11445
- Moneron, G. et al. Fast STED microscopy with continuous wave fiber lasers. Opt. Express 18, 1302-1309 (2010).
- Schneider, J. et al. Ultrafast, temporally stochastic STED nanoscopy of millisecond dynamics. Nat. Methods 12, 827-830 (2015).
- Beater, S., Holzmeister, P., Pibiri, E., Lalkens, B. & Tinnefeld, P. Choosing dyes for cw-STED nanoscopy using self-assembled nanorulers. Phys. Chem. Chem. Phys. 16, 6990-6996 (2014).
- 33. Han, K.Y. et al. Three-dimensional stimulated emission depletion microscopy of nitrogen-vacancy centers in diamond using continuous-wave light. Nano Lett. 9, 3323-3329 (2009).
- 34. Lesoine, M.D. et al. Subdiffraction, luminescence-depletion imaging of isolated, giant, CdSe/CdS nanocrystal quantum dots. J. Phys. Chem. C **117**, 3662-3667 (2013).
- 35. Liu, Y. et al. Amplified stimulated emission in upconversion nanoparticles for super-resolution nanoscopy. Nature 543, 229-233 (2017).
- Staudt, T. et al. Far-field optical nanoscopy with reduced number of state transition cycles. Opt. Express 19, 5644-5657 (2011).
- 37. Göttfert, F. et al. Strong signal increase in STED fluorescence microscopy by imaging regions of subdiffraction extent. Proc. Natl. Acad. Sci. USA 114, 2125-2130 (2017).
- 38. Heine, J. et al. Adaptive-illumination STED nanoscopy. Proc. Natl. Acad. Sci. USA 114, 9797-9802 (2017).
- 39. Danzl, J.G. et al. Coordinate-targeted fluorescence nanoscopy with multiple off states. Nat. Photonics 10, 122-128 (2016).

PERSPECTIVE

- Castello, M. et al. Gated-sted microscopy with subnanosecond pulsed fiber laser for reducing photobleaching. Microsc. Res. Tech. 79, 785-791 (2016).
- 41. Strack, R. Death by super-resolution imaging. Nat. Methods 12, 1111 (2015).
- Wäldchen, S., Lehmann, J., Klein, T., van de Linde, S. & Sauer, M. Lightinduced cell damage in live-cell super-resolution microscopy. Sci. Rep. 5, 15348 (2015).
- Laissue, P.P., Alghamdi, R.A., Tomancak, P., Reynaud, E.G. & Shroff, H. Assessing phototoxicity in live fluorescence imaging. *Nat. Methods* 14, 657–661 (2017).
- Hein, B., Willig, K.I. & Hell, S.W. Stimulated emission depletion (STED) nanoscopy of a fluorescent protein-labeled organelle inside a living cell. Proc. Natl. Acad. Sci. USA 105, 14271–14276 (2008).
- Schermelleh, L., Heintzmann, R. & Leonhardt, H. A guide to superresolution fluorescence microscopy. J. Cell Biol. 190, 165–175 (2010).
- Lukinavičius, G. et al. Fluorogenic probes for live-cell imaging of the cytoskeleton. Nat. Methods 11, 731–733 (2014).
- Lukinavičius, G. et al. SiR-Hoechst is a far-red DNA stain for live-cell nanoscopy. Nat. Commun. 6, 8497 (2015).
- Butkevich, A.N. et al. Fluorescent rhodamines and fluorogenic carbopyronines for super-resolution STED microscopy in living cells. Angew. Chem. Int. Ed. Engl. 55, 3290–3294 (2016).
- Lukinavičius, G. et al. A near-infrared fluorophore for live-cell super-resolution microscopy of cellular proteins. Nat. Chem. 5, 132–139 (2013).
- Matela, G. et al. A far-red emitting fluorescent marker protein, mGarnet2, for microscopy and STED nanoscopy. Chem. Commun. (Camb.) 53, 979–982 (2017).
- Opazo, F. et al. Aptamers as potential tools for super-resolution microscopy. Nat. Methods 9, 938–939 (2012).
- Shcherbakova, D.M. & Verkhusha, V.V. Chromophore chemistry of fluorescent proteins controlled by light. Curr. Opin. Chem. Biol. 20, 60–68 (2014).
- Hell, S.W. Toward fluorescence nanoscopy. Nat. Biotechnol. 21, 1347–1355 (2003).
- Friedrich, M., Gan, Q., Ermolayev, V. & Harms, G.S. STED-SPIM: stimulated emission depletion improves sheet illumination microscopy resolution. *Biophys. J.* 100, L43–L45 (2011).
- Gohn-Kreuz, C. & Rohrbach, A. Light-sheet generation in inhomogeneous media using self-reconstructing beams and the STED-principle. *Opt. Express* 24, 5855–5865 (2016).
- Chen, B.-C. et al. Lattice light-sheet microscopy: imaging molecules to embryos at high spatiotemporal resolution. Science 346, 1257998 (2014).
- Urban, N.T., Willig, K.I., Hell, S.W. & Nägerl, U.V. STED nanoscopy of actin dynamics in synapses deep inside living brain slices. *Biophys. J.* 101, 1277–1284 (2011).
- Patton, B.R., Burke, D., Vrees, R. & Booth, M.J. Is phase-mask alignment aberrating your STED microscope? Methods Appl. Fluoresc. 3, 024002 (2015).
- Loew, L.M. & Hell, S.W. Superresolving dendritic spines. Biophys. J. 104, 741–743 (2013).
- 60. Ke, M.-T. *et al.* Super-resolution mapping of neuronal circuitry with an index-optimized clearing agent. *Cell Rep.* **14**, 2718–2732 (2016).
- Unnersjö-Jess, D., Scott, L., Blom, H. & Brismar, H. Super-resolution stimulated emission depletion imaging of slit diaphragm proteins in optically cleared kidney tissue. Kidney Int. 89, 243–247 (2016).

- 62. Bingen, P., Reuss, M., Engelhardt, J. & Hell, S.W. Parallelized STED fluorescence nanoscopy. *Opt. Express* 19, 23716–23726 (2011).
- Yang, B., Przybilla, F., Mestre, M., Trebbia, J.-B. & Lounis, B. Large parallelization of STED nanoscopy using optical lattices. *Opt. Express* 22, 5581–5589 (2014).
- Bergermann, F., Alber, L., Sahl, S.J., Engelhardt, J. & Hell, S.W. 2000-fold parallelized dual-color STED fluorescence nanoscopy. *Opt. Express* 23, 211– 223 (2015).
- Kastrup, L., Blom, H., Eggeling, C. & Hell, S.W. Fluorescence fluctuation spectroscopy in subdiffraction focal volumes. *Phys. Rev. Lett.* 94, 178104 (2005).
- Eggeling, C. et al. Direct observation of the nanoscale dynamics of membrane lipids in a living cell. Nature 457, 1159–1162 (2009).
- Lanzanò, L. et al. Measurement of nanoscale three-dimensional diffusion in the interior of living cells by STED-FCS. Nat. Commun. 8, 65 (2017).
- Niehörster, T. et al. Multi-target spectrally resolved fluorescence lifetime imaging microscopy. Nat. Methods 13, 257–262 (2016).
- Donnert, G. et al. Two-color far-field fluorescence nanoscopy. Biophys. J. 92, L67–L69 (2007).
- Schmidt, R. et al. Spherical nanosized focal spot unravels the interior of cells. Nat. Methods 5, 539–544 (2008).
- Sidenstein, S.C. et al. Multicolour multilevel STED nanoscopy of actin/ spectrin organization at synapses. Sci. Rep. 6, 26725 (2016).
- Galiani, S. et al. Super-resolution microscopy reveals compartmentalization of peroxisomal membrane proteins. J. Biol. Chem. 291, 16948–16962 (2016).
- Sednev, M.V., Belov, V.N. & Hell, S.W. Fluorescent dyes with large Stokes shifts for super-resolution optical microscopy of biological objects: a review. Methods Appl. Fluoresc. 3, 042004 (2015).
- Lukinavičius, G. et al. Fluorogenic probes for multicolor imaging in living cells. J. Am. Chem. Soc. 138, 9365–9368 (2016).
- Tønnesen, J., Nadrigny, F., Willig, K.I., Wedlich-Söldner, R. & Nägerl, U.V. Two-color STED microscopy of living synapses using a single laser-beam pair. *Biophys. J.* 101, 2545–2552 (2011).
- Ringemann, C. et al. Exploring single-molecule dynamics with fluorescence nanoscopy. New J. Phys. 11, 103054 (2009).
- Ta, H. et al. Mapping molecules in scanning far-field fluorescence nanoscopy. Nat. Commun. 6, 7977 (2015).
- Harke, B., Chacko, J., Haschke, H., Canale, C. & Diaspro, A. A novel nanoscopic tool by combining AFM with STED microscopy. *Opt. Nanoscopy* 1, 3 (2012).
- Zanella, R. et al. Towards real-time image deconvolution: application to confocal and STED microscopy. Sci. Rep. 3, 2523 (2013).
- Hell, S.W. et al. The 2015 super-resolution microscopy roadmap. J. Phys. D Appl. Phys. 48, 443001 (2015).
- 81. Rankin, B.R. et al. Nanoscopy in a living multicellular organism expressing GFP. Biophys. J. 100, L63–L65 (2011).
- Meyer, L. et al. Dual-color STED microscopy at 30-nm focal-plane resolution. Small 4, 1095–1100 (2008).
- Coto Hernàndez, I., d'Amora, M., Diaspro, A. & Vicidomini, G. Influence of laser intensity noise on gated CW-STED microscopy. *Laser Phys. Lett.* 11, 095603 (2014).